

Microwave - assisted hydrothermal synthesis and characterization of hierarchical structured ZnO nanorods

H. LIU*, D. YANG, H. SUN, Z. ZHU

School of Materials Science and Engineering, Shaanxi University of Science and Technology, Xi'an 710021, P. R. China

Hierarchical structured ZnO nanorods with the whole diameter about ~ 400 nm and the length of $\sim 1\mu\text{m}$ have been synthesized by a simple microwave-assisted hydrothermal method. X-ray diffraction (XRD) analysis, scanning electron microscopy (SEM), transmission electron microscopy (TEM), Fourier transform infrared (FT-IR) spectroscopy and X-ray photoelectron spectrometer (XPS) was used for characterization of as-prepared products. On the surface of the as-prepared ZnO nanorods, thornlike nanostructures with the diameter and length of 20~100 nm and ~ 20 nm are developed in a large density. The possible growth mechanism of this hierarchical structured nanorod may be attributed to the formation of the ZnO nanorods with the help of the linear template agent and the following nucleation and growth of the thornlike nanostructures in the defect sites of the ZnO nanorods. The photocatalytic experiment results shown that the as-prepared ZnO hierarchical structured nanorods exhibit excellent photocatalytic activity because of their special morphology and structure.

(Received June 7, 2010; accepted October 14, 2010)

Keywords: Nanostructures materials; Oxide materials; Chemical synthesis, ZnO, TEM, XRD, SEM

1. Introduction

Morphology-controlled synthesis of desired micro/nanostructures from nanosized building blocks has received considerable attention because the physical and chemical properties of micro/nanostructured materials including optical, electronic, magnetic, and catalytic properties are strongly related not only to their size but also to their morphology [1]. Comparing with the size control, the morphology control is more demanding to achieve by means of adding additives. Although it has already been tried for long time, the knowledge about influence crystal morphology is still limited. The architectural control of nanocrystals with well-defined shapes is an important goal of modern materials science because of the importance of the shape and texture of materials in determining their widely varying properties [2]. Specifically, many recent efforts have been devoted to the hierarchical micro/nanostructured materials, which possess dual or multiple morphologies and structures, for fully understanding dimensionally confined transport phenomena in functional oxides and for building functional devices.

Several kinds of hierarchical micro/nanostructured materials have been synthesized, such as Cu_2O [3], WO_3 [4], TiO_2 [5], SiO_2 [6], Fe_2O_3 [7], and ZnO [8, 9]. Among these, ZnO nanomaterials, as one of important semiconductor materials, have been investigated widely for their catalytic, electrical, optoelectronic, and photochemical properties. Novel hierarchical micro/nanostructured ZnO materials may find applications in a variety of fields that require not only high surface area but also structural integrity. Up to now, the synthetic approaches for the hierarchical micro/nanostructured ZnO materials can be generally classified into two categories:

vapor-phase growth [10] and solution-phase growth [11]. However, the control of the regularity for hierarchical micro/nanostructured ZnO materials is a challenging task, and the regularity is now commonly controlled by metal catalyst through the vapor-liquid-solid mechanism [12]. In comparison to the complex thermal evaporation technique, the solution-based process for the formation of the hierarchical micro/nanostructured ZnO materials has received broad attention in recent. Liu's group demonstrated a wet-chemical route for the synthesis of ZnO hierarchical structured nanorods which possessing excellent optical and gas sensing properties simultaneously [13]. Tong et al. reported the preparation of nanosheet-assembled quasi-sphere-like ZnO by ice-water bath and reflux steps, and the obtained hierarchical nanostructured ZnO shown significantly improved photocatalytic activity [14]. However, all these solution-based approaches are time expensive or complex, which limited the mass production and potential applications of these hierarchical structured ZnO materials. Herein, we report a simple and time inexpensive microwave-assisted hydrothermal route for the preparation of ZnO hierarchical nanostructures. The as-obtained products exhibit excellent photocatalytic property because of their special morphology and structure. Besides, the method can be extended to other similar metallic oxide hierarchical structured materials for specific applications.

2. Experimental section

2.1 Preparation of hierarchical nanostructured ZnO nanorods

Hierarchical nanostructured ZnO nanorods were fabricated via a microwave-assisted hydrothermal method.

All chemical reagents were analytical grade and used without further purification. In a typical synthesising process, 1.0 mmol poly ethylene glycols (PEG)-2000, which was employed as a soft surfactant template for orientating crystal growth, was dissolved in a solution consisting of 50.0 mL of ethanol and 10.0 mL distilled water with vigorous stirring by a magnetic stirrer. The solution is marked as solution A. Meanwhile, 3.0 mmol $\text{Zn}(\text{NO}_3)_2 \cdot 6\text{H}_2\text{O}$ and 0.06 mol NaOH were dissolved in 5.0 mL distilled water under constant stirring. This solution was called as solution B. The mixture of solution A and B experienced a 10 min supersonic (40KHz) pretreatment in a pulverizer with a power of 400W and then was transferred into a Teflon-lined autoclave with a capacity of 100.0 mL. The autoclave was treated at 180°C for 30 min under temperature-controlled mode in a MDS-8 microwave hydrothermal system. After reaction, the autoclave was allowed to cool to room temperature naturally. Then the as-prepared white precipitates were alternatively washed with distilled water and absolute alcohol for several times, respectively. Finally, the white precipitates were dried in a vacuum oven at 80°C for 12h and the sample was obtained.

2.2 Characterization

The morphology and structure of the as-prepared samples were characterized by using JEOL JSM-6700F field-emission scanning electron microscopy (FESEM) equipped with energy dispersive X-ray analysis (EDX), D/max2200pc X-ray diffractometer (XRD) with $\text{Cu K}\alpha$ radiation (1.5418Å), JEOL JEM-2010 high-resolution transmission electron microscopy (HRTEM) at an accelerating voltage of 200KV, respectively. Element analysis was carried out on an ESCALab MK II X-ray photoelectron spectrometer (XPS) using noomonochromatized $\text{Mg K}\alpha$ X-ray as the excitation source. Fourier transform infrared (FT-IR) spectrometer (Bruker, FTIR-V 70, German) was used for detection of the as-obtained ZnO products and the calcined samples. The degradation process was analyzed by monitoring dye absorption intensity at the maximum absorption wavelength using a UV/Vis/NIR spectrometer (Perkin Elmer, Lambda 950).

2.3 Photo-degradation test procedures

All photoreactions were carried out in glass breakers (capacity ~100mL). Each contained 20 mL Rhodamin B aqueous solution (1.25mg l^{-1}) and 10mg of the as-prepared ZnO nanostructures as photocatalysts. The reaction system was sonicated for 30 min to reach adsorption equilibrium of dye. After that, the reaction system was placed about 10 cm below the 365 nm light source of a UV lamp (WFH-203, 220 V, 50 Hz), and irradiated for different periods in dark at room temperature. The whole reaction proceeded under magnetic stirring. The efficiency of the degradation processes was analyzed by monitoring dye decolorization at the maximum adsorption wavelength, using a UV/Vis/NIR spectrometer. Photocatalysts were then separated from solutions via simple filtering, rinsed with ethanol to fully remove the residual organic species, and reused for next run.

3. Results and discussion

The morphology and structure of the as-grown products are revealed by the typical FESEM and TEM images, as shown in images a and b in Figure 1, respectively. Thornlike nanostructures grown on the surface of uniform hierarchical structured ZnO nanorods in high density have length of ca. 20~100 nm and approximately in diameter of 20 nm, respectively. The diameter and length of the the entire hirarchical structured nanorods is about 400 nm and 1 μm , respectively. While some of the nanorods assembled to a ZnO quasi-micorsphere, similar to that reported in the literature without the template and surfactant [15]. The chemical composition of the as-obtained products was observed using EDX measurements. Figure 1c shows the typical EDX spectrum of the hierarchical nanostructures indicting that the grown structures are composed from zinc and oxygen with approximate stoichiometry of ZnO without other impurities.

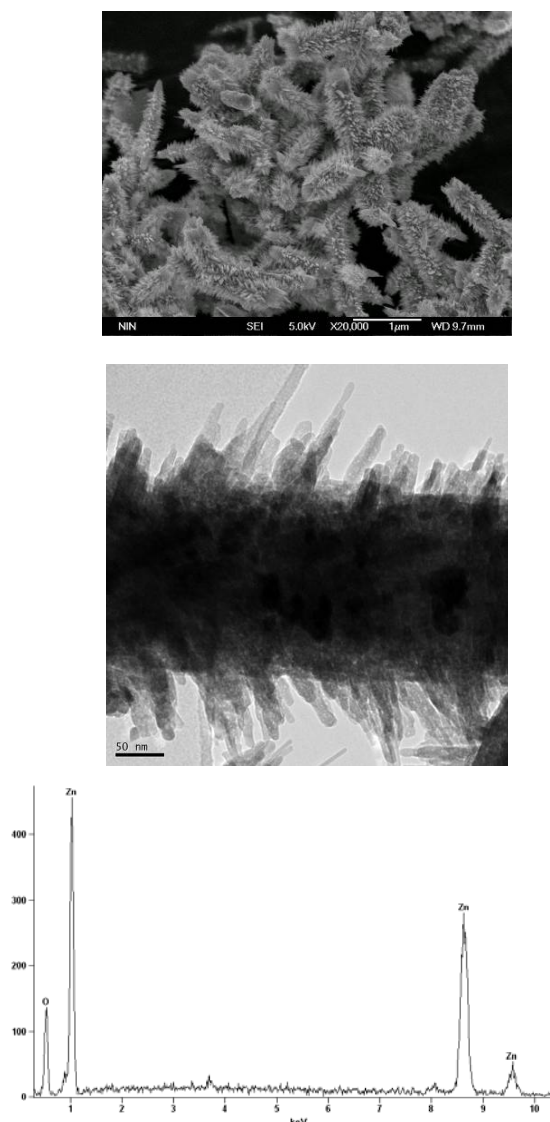


Fig. 1 (a) FESEM micrograph, (b) TEM image, and (c) EDX spectrum of the as-obtained products.

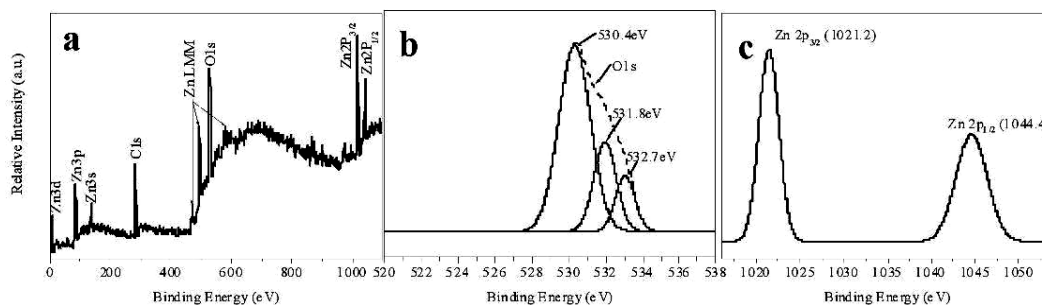


Fig. 2. XPS spectra of the as-prepared samples: (a) survey spectrum, (b) O 1s spectrum, and (c) Zn 2p_{3/2} and Zn 2p_{1/2} spectrum.

The composition and purity of the as-grown samples were also confirmed by XPS, as presented in Fig. 2. The peaks of Zn and O can be clearly observed in the survey spectrum (Figure 2a) without other impurities (the appearance of C can be attributed to the adsorbed CO₂ on the surface of samples in air). From the survey spectrum, we can conclude that the product is pretty pure, which is in good agreement with the result of EDX. In the high resolution spectrum for O regions (Figure 2b), peaks located at 530.4, 531.8, and 532.7 eV can be indexed to O²⁻ from wurtzite-typed ZnO structure, ZnO crystal where O is insufficient, and adsorbed H₂O in air, respectively [16, 17]. See from panel c in Fig. 2, the binding energy is 1021.2 eV for Zn 2p_{3/2}, as well as 1044.4 eV for Zn 2p_{1/2}, respectively. Quantification of peaks gives a ratio of Zn to O of 1.02:1.00, which is closely consistent with the stoichiometry of ZnO.

Fig. 3 shows the XRD pattern of the as-grown hierarchical structured nanorods. The diffraction peaks can be indexed to hexagonal wurtzite-typed ZnO with lattice constants of $a=0.3249$ nm and $c=0.5206$ nm (JCPDS card: 36-1451). No diffraction peaks from either ZnO or other phases or impurities are detected. The results of XRD correspond with the XPS analysis well. Figure shows the XRD patterns of as-synthesized samples at 180°C for different holding times, respectively.

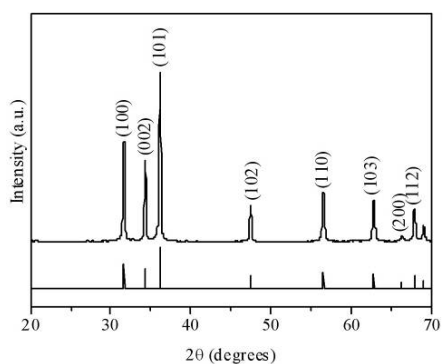


Fig. 3. XRD patterns of hierarchical structured ZnO nanorods. The vertical lines at the bottom correspond to the standard XRD pattern of wurtzite-typed ZnO (JCPDS No. 36-1451).

In order to further indentified the delicate surface morphology and structure of the as-grown ZnO nanorods, the typical TEM images of an individual hierarchical structured ZnO nanorod and high-magnification of the thornlike branch were shown in Fig. 4. It can be seen that

the thorn-like nanostructure grown on the surface of nanorods in high density have different length from ca. 20 nm to 80 nm, and approximately in diameter of ~20 nm. Fig. 4(b) shows the high resolution TEM (HRTEM) image of the grown thornlike nanostructures confirms that these structures are single crystalline and grown along the [002] direction. The lattice spacing, corresponding to the d -spacing of [002] crystal planes of the wurtzite ZnO, is 0.26 nm for the grown nanorods confirming that the grown nanostructures are preferentially oriented in the c -axis direction. The inset in Figure 4(b) is a typical selected-area electron diffraction (SAED) pattern taken from this individual thornlike nanostructure. The diffraction spots in this pattern form rectangular arrays and can be indexed to crystal planes (0110) and (0001). The results reveal that the thornlike nanostructures are single crystal in nature and possess hexagonal ZnO phase grown along the c -axis direction, consistent with the above-mentioned result from XRD.

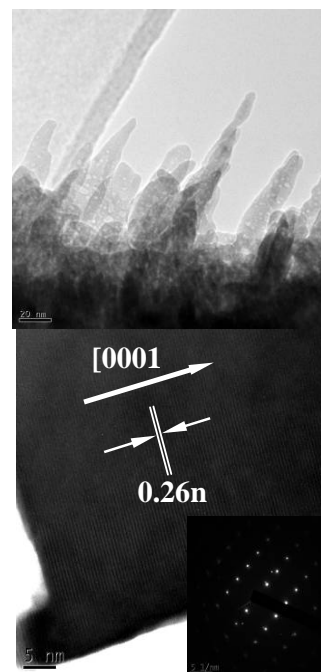


Fig. 4. (a) HRTEM of an individual hierarchical structured ZnO nanorod; (b) High-magnification lattice-resolved images and SAED pattern (inset) from a thornlike branch.

Fig. 5 shows the FT-IR spectrum of the as-prepared samples and ZnO obtained by calcination at 500°C. Curve a in Figure 5 is the FT-IR spectrum of the as-prepared samples. The majority of infrared absorption peaks are located in the middle and lower frequencies zones. The hydroxyl groups and water molecules are confirmed by the broad bands detected at high frequency at around 3412 cm^{-1} . The peaks at 1109, 842, 719, and 484 cm^{-1} belong to C-O-C and $-\text{CH}_2-$ vibration, which originate from surfactant of PEG. The peaks at around $\sim 2883 \text{ cm}^{-1}$ are attributed to the asymmetric and symmetric stretching vibrations of $-\text{CH}_2$ group [18, 19]. The band at 1460 cm^{-1} can be attributable to the non-structural carbonate group. All of these peaks are not observed in curve b, which indicate the complete elimination of the PEG surfactant. Curve b in Figure 5 is the FT-IR spectrum of the ZnO obtained by calcination at 500°C. The broad absorption bands at ~ 3416 and $\sim 1617 \text{ cm}^{-1}$ are still in existence, which can be assigned to O-H bending vibrations of adsorbed water molecules on ZnO particles or on KBr wafers [20]. The absorption bands of 400–500 cm^{-1} are attributed to the stretching vibrations of ZnO. However, the characteristic peak splits into two peaks, which may be associated with the special structure of the obtained ZnO hierarchical nanorods. The polarity of nanocolumns is stronger than that of the spherical particles. Thus, the increase of stretching polarity of the ZnO band results in great splitting of the ZnO characteristic peak [21, 22].

To understand the growth mechanism of hierarchical nanostructures, we also carried out a series of synthetic reactions at temperature of 180°C with different times. Figure 6 shows the morphology of products obtained at different reaction times.

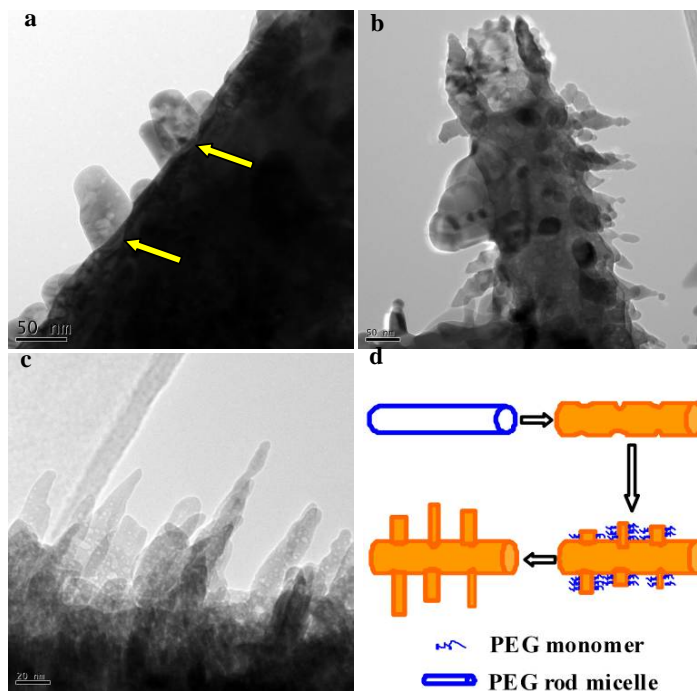


Fig. 6. Morphology of ZnO nanostructures grown at 180°C for (a) 10 min, (b) 20 min, and (c) 30 min, respectively. (d) schematic diagram of the formation mechanism of the ZnO hierarchical nanostructures.

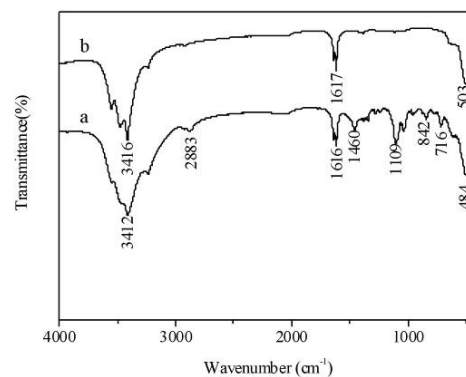


Fig. 5. FT-IR spectrum of the as-prepared samples (Curve a) and ZnO obtained by calcination at 500°C (Curve b).

The initial formation of hierarchical structure is revealed by the morphology of ZnO nanorods grown at 180°C for about 10 min, as shown in Figure 6a. Through the 10 min hydrothermal reaction, the rod-like ZnO has already been formed. At the same times, a short thornlike ZnO appears at the defect sites, shown as the yellow arrows in Figure 6a. Different with that reported by Liu and his coworkers [13], the surface of the ZnO nanorods is firstly covered with a large quantity of sheetlike nanostructures, and then developed as the thornlike structures with the increase of the hydrothermal reaction temperature. In this work, the thornlike structures formed directly at the initial times.

With the increasing of the hydrothermal reaction times, more and more thornlike structures appear at the surface of the ZnO nanorod and become longer, shown as Figure 6 a and b. As a result, the hierarchical structure is formed with thornlike structures assembling in disorder on the surface of trunklike ZnO nanorods. This growth mechanism is similar to the report by Wang's group, in which two growth stages were proposed, i.e., nucleation and subsequent epitaxial growth [23]. Figure 6d show the schematic diagram of the formation mechanism of the ZnO hierarchical nanostructures. Firstly, the one-dimensional ZnO nanorod is formed with the help of the linear PEG template agent at the initial hydrothermal reaction period [24]. Then, the growth of nanostructured branches is excited at the defect sites, which are produced during the formation of ZnO nanorods. In other words, the defects, e.g., stacking faults and twins, act as seeds for epitaxial growth of the thornlike structures. Secondly, the crystal lattice planes with fast growth rate develop dominantly, resulting in the thornlike profile. In this stage, the absorbed PEG in the surface of the thornlike structures promoted its epitaxial growth.

The photocatalytic activities of as-prepared ZnO hierarchical nanorods were carried out using UV light and visible light. Rhodamin B was used as a test contaminant since it has been extensively used as an indicator for photocatalytic activities [25] owing to its absorption peaks in the visible range. Figure 7 shows the variation in the UV-Vis absorption spectrum of dye molecules at different intervals for Rhodamin B. It can be clearly seen that the maximum absorbance at 554 nm disappears almost completely after irradiation for about 6 hours. Since no new peaks were observed during the whole process for this dye, a degradation reaction has occurred. The photocatalytic activity of this ZnO hierarchical nanostructures can be attributed both to the donor states caused by the large number of defect sites such as oxygen vacancies and interstitial zinc atom and to the acceptor states which arise from zinc vacancies and interstitial oxygen atoms [26].

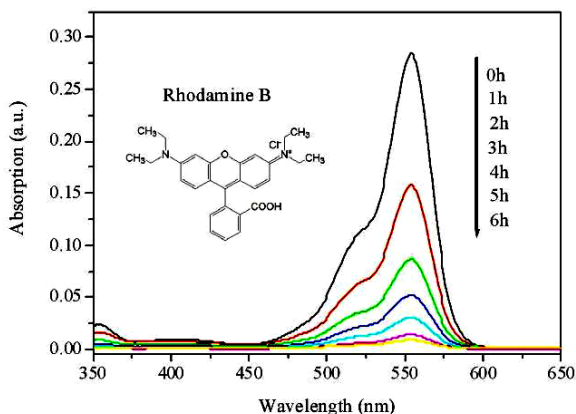


Fig. 7. Variation of the absorption spectrum for Rh B in the presence of ZnO hierarchical nanostructures under irradiation with UV light at different intervals.

4. Conclusions

Novel hierarchical structured ZnO nanorods with single-crystalline thornlike nanostructures grown on the surface in large density have been successfully fabricated via simple and time inexpensive microwave assisted hydrothermal route. The diameter and length of the entire hierarchical structured nanorods is about 400 nm and 1 μm , respectively. The thornlike nanostructures grown on the surface of ZnO nanorods have the length of ca. 20~100 nm and approximately in diameter of 20 nm, respectively. The growth mechanism is suggested from two aspects: the formation of the ZnO nanorods with the help of the linear PEG template agent and the following nucleation and growth of the thornlike nanostructures in the defect sites of the ZnO nanorods. The photocatalytic experiment results shown that the as-prepared ZnO hierarchical nanorods exhibit excellent photocatalytic activity because of their special morphology and structure. The ZnO nanomaterials with hierarchical nanostructures enable them to be potential candidates as building blocks for the development of novel functional optoelectronic devices. Besides, the method can be extended to other similar metallic oxide hierarchically structured materials for specific applications.

Acknowledgements

This work was financially supported by the China Postdoctoral Science Foundation Founded Project (No. 20080440185, 200902584), the Special Found form Shaanxi Provincial Department of Education (09JK355), and the National Science Foundation of China (No. 50772064).

Reference

- [1] J. S. Bradley, B. Tesche, W. Busser, M. Masse, M. T. Reetz. *J. Am. Chem. Soc.* **122**, 4631(2000).
- [2] Y. Ma, L. Qi, J. Ma, H. Cheng, *Growth Des.* **4**, 351 (2004).
- [3] H. R. Liu, W. F. Miao, S. Yang, Z. M. Zhang, J. F. Chen. *Cryst. Growth Des.* **9(4)**, 1733(2009).
- [4] M. Shibuya, M. Miyauchi. *Chem. Phys. Lett.* **473**, 126(2009).
- [5] X. Dong, J. Tao, Y. Y. Li, H. Zhu. *Appl. Surf. Sci.* **255**, 7183(2009).
- [6] Z. Pan, S. Dai, D. B. Beach, D. H. Lowdes. *Nano Lett.* **3**, 3159(2003).
- [7] T. Yu, B. Varghese, Z. X. Shen, C. T. Lim, C. H. Sow. *Mater. Lett.* **62**, 389(2008).
- [8] X. P. Gao, Z. F. Zheng, H. Y. Zhu, G. L. Pan, J. L. Bao, F. Wu, D. Y. Song. *Chem. Commun.* **8**, 1428(2004).
- [9] C. Y. Kuan, J. M. Chou, I. C. Leu, M. H. Hon. *Journal of Solid State Chemistry*, **181**, 673(2008).

- [10] Z. R. Dai, Z. W. Pan, Z. L. Wang. *Adv. Funct. Mater.* **13**, 9 (2003).
- [11] L. Vayssieres, K. Keis, S. E. Lindquist, A. Hagfeldt. *J. Phys. Chem. B* **105**, 3350(2001).
- [12] K. A. Dick, K. Deppert, M. W. Larsson, T. Martensson, W. Seifert, L. R. Wallengera, L. Samuelson. *Nat. Mater.* **3**, 380(2004).
- [13] J. Y. Liu, Z. Guo, F. L. Meng, Y. Jia, T. Luo, M. Q. Li, J. H. Liu. *Cryst. Growth Des.* **9(4)**, 1716(2009).
- [14] Y. H. Tong, J. Cheng, Y. L. Liu, and G. G. Siu. *Script Materialia* **60**, 1093(2009).
- [15] X. F. Zhou, D. Y. Zhang, Y. Zhu, Y. Q. Shen, X. F. Guo, W. P. Ding, Y. Chen. *J. Phys. Chem. B* **110**, 25734(2006).
- [16] Y. Du, M. S. Zhang, J. Hong, Y. Shen, Q. Chen, Y. Yin. *Appl. Phys. A: Mater. Sci. Process* **76**, 171(2003).
- [17] R. J. Cebulla. *Appl. Phys.* **83**, 171(1998).
- [18] Z. F. Liu, Z. G. Jin, W. Li, J. J. Qiu. *Mater. Lett.* **59**, 3620(2005).
- [19] R. Y. Hong, T. T. Pan, J. Z. Qian, H. Z. Li. *Chem. Engin. J.* **119**, 71(2006).
- [20] S. Musić, S. Popović, M. Maljković, D. Dragčvić. *J. alloys Compd.* **347**, 324(2002).
- [21] X. C. Li, G. H. He, G. K. Xiao, H. J. Liu, M. Wang. *J. Colloid and Interface Science* **333**, 465(2009).
- [22] S. Musić, A. Šarić, S. Popović. *J. Alloys Compd.* **448**, 277(2008).
- [23] P. Jiang, J. J. Zhou, H. F. Fang, C. Y. Wang, Z. L. Wang, S. S. Xie. *Adv. Funct. Mater.* **17**, 1303(2007).
- [24] X. M. Hou, F. Zhou, B. Yu, W. M. Liu. *Mater. Lett.* **61**, 2551(2007).
- [25] M. A. Rauf, S. S. Ashraf. *Chem. Engin. J.* **151**, 10(2009).
- [26] F. Tuomisto, K. Saarinen. *Phys. Rev.* **71**, 085206-1(2005).

*Corresponding author: liuhui@sust.edu.cn